Thyroid hormone receptor α mutation causes a severe and thyroxine-resistant skeletal dysplasia in female mice

J.H. Duncan Bassett[1], Alan Boyde[2], Tomas Zikmund[3], Holly Evans[4], Peter I. Croucher[5], Xuguang Zhu[6], Jeong Won Park[6], Sheue-yann Cheng[*6], Graham R. Williams[*1]

[1]Department of Medicine, Imperial College London, UK; [2]Dental Physical Sciences, Oral Growth and Development, Queen Mary University of London, UK; [3]Laboratory of X-Ray Micro-CT and Nano-CT, Central European Institute of Technology, Brno University of Technology, Czech Republic; [4]Sheffield Myeloma Research Team, University of Sheffield, UK; [5]Bone Biology Program, Garvan Institute of Medical Research, Sydney, Australia; [6]Laboratory of Molecular Biology, National Cancer Institute, Bethesda, USA

A new genetic disorder has been identified that results from mutation of *THRA*, encoding thyroid hormone receptor α1 (TRα1). Affected children have a high serum T3/T4 ratio and variable degrees of intellectual deficit and constipation, but exhibit a consistently severe skeletal dysplasia. In an attempt to improve developmental delay and alleviate symptoms of hypothyroidism, patients are receiving varying doses and durations of T4 treatment but responses have been inconsistent so far. *Thra1*$^{PV/+}$ mice express a similar potent dominant-negative mutant TRα1 to affected individuals, and thus represent an excellent disease model. We hypothesized that *Thra1*$^{PV/+}$ mice could be used to predict the skeletal outcome of human *THRA* mutations and determine whether prolonged treatment with a supra-physiological dose of T4 ameliorates the skeletal abnormalities. Adult female *Thra1*$^{PV/+}$ mice had short stature, grossly abnormal bone morphology but normal bone strength despite high bone mass. Although T4 treatment suppressed TSH secretion, it had no effect on skeletal maturation, linear growth or bone mineralization, thus demonstrating profound tissue resistance to thyroid hormone. Despite this, prolonged T4 treatment abnormally increased bone stiffness and strength, suggesting the potential for detrimental consequences in the long-term. Our studies establish that TRα1 has an essential role in the developing and adult skeleton, and predict that patients with different *THRA* mutations will display variable responses to T4 treatment, which depend on the severity of the causative mutation.

The *THRA* and *THRB* genes encode the nuclear receptors TRα and TRβ, which mediate thyroid hormone action in target tissues (1). Autosomal dominant resistance to thyroid hormone (RTH) was recognized in 1967 (2), and the first causative mutations affecting *THRB* were identified 22 years later (3). Over 1000 RTH families have since been described, and affected individuals have increased thyroid hormone levels with an inappropriately normal or elevated thyroid stimulating hormone (TSH) concentration due to disruption of the hypothalamus-pituitary-thyroid (HPT) axis (4).

After the identification of *THRB* mutations in individuals with RTH it was a further 23 years before the first *THRA* mutations were reported in 2012 and 2013 (5–7). A six year-old girl with skeletal dysplasia and growth retardation was found to have a heterozygous *THRA* non-

Abbreviations:

ISSN Print 0013-7227 ISSN Online 1945-7170
Printed in U.S.A.

Received December 19, 2013. Accepted April 11, 2014.

sense mutation resulting in expression of a truncated TRα1^{E403X} protein. She had normal serum TSH with low/normal thyroxine (T4) and high/normal 3,5,3′-L-triiodothyronine (T3) concentrations. Further investigations revealed macrocephaly with patent and abnormal skull sutures, delayed tooth eruption and bone age, disproportionate short stature, and epiphyseal dysgenesis with delayed mineralization of secondary ossification centers. Treatment with T4 for nine months resulted in suppression of TSH and an increased basal metabolic rate, but did not improve linear growth or skeletal development (5). A second girl with similar thyroid function and skeletal dysplasia was found to have a heterozygous frameshift mutation in *THRA* resulting in expression of a truncated TRα1^{F397fs406X} protein (6). She presented at the age of three with macrocephaly, delayed tooth eruption, absent secondary ossification centers and congenital hip dislocation. Reducing growth velocity became evident between three and six years of age. T4 treatment between six and eleven years of age only resulted in a small increase in growth velocity for a two month period but ultimately had no effect on her height, which continued along the 20th centile and was accompanied by persistently delayed bone age. The girl's 47 year-old father had the same *THRA* mutation and displayed short stature with a height 3.77SD below normal and acquired hearing loss due to otosclerosis (6, 8). Recently, a 45 year-old female with similar thyroid function, macrocephaly and disproportionate short stature was identified and found to have a heterozygous frameshift mutation in *THRA* resulting in expression of a truncated TRα1^{P382fs388X} protein. She presented in infancy with developmental delay and was treated intermittently with T4, which resulted in some improvement in growth velocity although her final adult height remained 2.34SD below normal (7).

These recent reports define a new genetic disorder characterized by a severe developmental phenotype with profound skeletal abnormalities that are thought to result from impaired T3 action in bone and cartilage (5–8). In an attempt to ameliorate the phenotype, three children have already received intermittent thyroxine at different doses and for varying durations. However, responses to date have been limited, and it is unknown whether long-term T4 treatment will be beneficial or detrimental. Thus, it is now essential to define the adult skeletal consequences of *THRA* mutations and determine the long-term effects of T4 supplementation, since life-long therapy is likely to be required. Importantly, Van Mullem et al showed that dominant-negative inhibition of TRβ by TRα1^{F397fs406X} in vitro could be overcome partially by a high concentration of thyroid hormone (8). Furthermore, several studies have demonstrated that TRβ may mediate T3 actions in bone and cartilage (9–12), even though the principal physiological effects are mediated by TRα1. These observations suggest, therefore, that treatment of patients with supra-physiological doses of T4 may improve their skeletal abnormalities via TRβ-mediated actions. To address this timely question we investigated the effects of prolonged T4 treatment in a mouse model of this novel disease.

Mice with dominant-negative mutations affecting *Thra* (*Thra1*^{PV}) and *Thrb* (*Thrb*^{PV}) were generated to investigate the tissue-specific roles of TRα and TRβ and aid the identification of patients with *THRA* mutations (13, 14). The PV mutation, first recognized in a patient with RTH, is a C-insertion in exon 10 of *THRB* that results in a frameshift affecting the C-terminal 16 amino acids (15). The equivalent *Thra1*^{PV} mutation comprises a homologous C-insertion followed by the PV sequence described in *THRB*^{PV} (14, 16). The *Thra1*^{PV} mutation disrupts helix 12 of TRα1, which is essential for T3 binding and coactivator recruitment (17), and lies within a 21 amino acid region containing the described human *THRA* mutations (5–7). Accordingly, TRα1^{PV} cannot bind T3 or activate target gene transcription, but acts as a potent dominant-negative inhibitor of wild type TRα1 or TRβ (14, 18, 19). Thus, the functional characteristics of TRα1^{PV} closely resemble those reported for TRα1^{E403X}, TRα1^{F397fs406X} and TRα1^{P382fs388X} (5–7). Importantly, PV and none of the described human mutations affect the sequence of the TRα2 isoform that is also expressed from the *THRA* locus but which cannot bind T3 and has no known physiological function. Consistent with this, juvenile *Thra1*$^{PV/+}$ mice display the same characteristics as children with heterozygous *THRA* mutations. They have a reduced T4:T3 ratio (14), delayed closure of the skull sutures with enlarged fontanelles and severe postnatal growth retardation with delayed bone age. These abnormalities result from impaired TRα1-mediated T3 action in bone and cartilage (20–22) indicating that *Thra1*^{PV} mice represent an excellent disease model in which to investigate the consequences of prolonged T4 treatment.

We hypothesized that the adult phenotype of *Thra1*$^{PV/+}$ mice would predict the skeletal outcome of human *THRA* mutations and determine whether affected individuals may be susceptible to fracture or osteoarthritis, both of which are associated with altered thyroid hormone action in bone (23–26). We also hypothesized that prolonged treatment of *Thra1*$^{PV/+}$ mice with a supra-physiological dose of T4 would ameliorate the developmental skeletal phenotype and improve bone structure and strength in adulthood.

The current studies demonstrate that adult *Thra1*$^{PV/+}$ mice have short stature but normal bone strength despite

high bone mass, suggesting that patients with *THRA* mutations are unlikely to have an increased risk of fracture. By contrast, gross morphological abnormalities of the bones and joints predict that individuals with *THRA* mutations may be predisposed to osteoarthritis (27, 28). Although treatment with a supra-physiological dose of T4 completely suppressed TSH secretion, it had no effect on skeletal maturation, linear growth or bone mineralization, thus demonstrating profound tissue resistance to thyroid hormone in *Thra1*$^{PV/+}$ mice. However, prolonged T4 treatment increased bone stiffness and strength abnormally due to progressive enlargement of cortical bone diameter and thickness. Overall, the findings suggest that T4 treatment of individuals with dominant-negative *THRA* mutations is unlikely to improve their skeletal abnormalities substantially and may even be detrimental in the long-term. Nevertheless, *Thra1*$^{PV/+}$ mice represent an important disease model in which to identify and evaluate new therapeutic approaches.

Materials and Methods

Thra1^{PV} mice

WT and heterozygous *Thra1*$^{PV/+}$ mice have a mixed C57BL/6J and NIH Black Swiss genetic background and were bred and genotyped as described (14, 21). Detailed characterization of the adult skeleton in *Thra1*$^{PV/+}$ mice was performed in 14 week-old female mice after cessation of growth, and in fully mature 20 week-old female mice that had been treated with vehicle or T4 from weaning at 4 weeks of age until sacrifice. All mice were given intra-peritoneal injections of calcein (10 mg/kg in 100μl PBS) 14 and 7 days before sacrifice (29).

Ethics

Animal studies were performed according to the National Institutes of Health Guide for Care and Use of Laboratory Animals, and the National Cancer Institute Animal Care and Use Committee granted ethical approval for all experiments.

Manipulation and measurement of thyroid status

TSH, T4, and T3 levels were determined in serum from mice (n = 5–13 per group) treated with vehicle or T4 (1.2 μg/ml in the drinking water) between 4–20 weeks of age. T4-supplemented water was changed every 3 days, with the T4 concentration adjusted to intake in two-week cycles to ensure all animals received the same amount of T4 and did not become markedly thyrotoxic (14, 30–32).

Histology

Tibias were fixed in 10% neutral buffered formalin and decalcified in 10% EDTA, embedded in paraffin wax. 5 μm sections were stained with alcian blue and van Gieson (29, 33). Measurements from at least four separate positions across the growth plate were obtained to calculate the mean height using a Leica DM LB2 microscope and DFC320 digital camera (Leica Microsystems, Milton Keynes, Buckinghamshire, UK). Results from 2 levels of sectioning were compared.

Faxitron digital x-ray microradiography

Femurs were imaged at 10 μm resolution using a Faxitron MX20 (Qados, Cross Technologies plc, Berkshire, UK). Bone mineral content (BMC) was determined relative to steel, aluminum and polyester standards. Images were calibrated with a digital micrometer and bone length, cortical bone diameter and thickness determined (33, 34).

Micro-CT

Femurs were analyzed by micro-CT (Skyscan 1172a) at 50 kV and 200 μA with a detection pixel size of 4.3 μm^2 and images were reconstructed using Skyscan NRecon software. A 1 mm^3 region of interest was selected 0.2 mm from the growth plate, and trabecular bone volume as proportion of tissue volume (BV/TV), trabecular number (Tb.N) and trabecular thickness (Tb.Th) determined (29, 33). Representative femurs from each treatment group were rescanned using a SCANCO μCT 40 (SCANCO Medical AG, Brüttisellen, Switzerland) operating at 55kVp peak energy detection, 6 μm resolution to obtain approximately 2500 cross-sections per specimen in 766 × 763 pixel 16 bit DICOM files. Raw data was imported using 32-bit Drishti v2.0.221 (Australian National University Supercomputer Facility, http://anusf.anu.edu.au/Vizlab/drishti/) and rendered using 64-bit Drishti v2.0.000 to generate high-resolution images.

Back scattered electron-scanning electron microscopy (EM) (BSE-SEM)

Femurs were fixed in 70% ethanol and opened longitudinally (33). Carbon-coated samples were imaged using backscattered electrons with a Zeiss DSM962 digital scanning electron microscope (EM) at 20 kV beam potential (KE Electronics, Toft, Cambridgeshire, UK). High-resolution images were quantified using ImageJ to determine the fraction of trabecular and endosteal bone surfaces displaying osteoclastic resorption (33).

Quantitative BSE-SEM (qBSE-SEM)

Bone mineralization was determined by qBSE-SEM at 1 μm^3 resolution. Specimens were embedded in methacrylate and block faces polished to an optical finish for SEM analysis at 20 kV, 0.5nA with a working distance of 11 mm (33). Gradations of micromineralization density were represented in eight equal intervals by a pseudocolor scheme (33, 35).

Osteoclasts

Sections from decalcified tibias were stained for tartrate resistant acid phosphatase (TRAP), counterstained with aniline blue, and imaged using a Leica DM LB2 microscope and DFC320 digital camera (29, 33). A montage of nine overlapping fields covering an area of 1 mm^2 located 0.2 mm below the growth plate was constructed for each bone. BV/TV was measured, and osteoclast numbers (Oc.N) and surface (Oc.S) determined in trabecular bone normalized to total bone surface (BS) (29, 33).

Osteoblasts

Methacrylate-embedded specimens were imaged with a Leica SP2 reflection confocal microscope at 488nm excitation to determine the fraction of bone surface undergoing active bone formation (33, 36). Mineral apposition rate (MAR) was calculated by determining the separation between calcein labels at 20 locations per specimen beginning 0.2 mm below the growth plate. BS and mineralizing surface (MS) were measured using ImageJ and the bone formation rate (BFR) calculated by multiplying MS and MAR.

Bone strength

Three-point bend tests were performed on tibias, with a constant rate of displacement of 0.03 mm/s until fracture, using an Instron 5543 load frame and 100N load cell (Instron Limited, High Wycombe, Buckinghamshire, UK). Biomechanical variables reflecting cortical bone strength were derived from load displacement curves (33, 37).

Statistics

Data were analyzed by unpaired two-tail student's t test; P values < 0.05 were considered significant. Frequency distributions of mineralization densities obtained by Faxitron and qBSE were compared using the Kolmogorov-Smirnov test (29, 33, 34).

Results

Thyroid status and response to T4 administration in Thra1$^{PV/+}$ *mice*

The thyroid status of adult WT and *Thra1*$^{PV/+}$ mice was determined following treatment with vehicle or a supra-physiological dose of T4 from weaning until 14 weeks of age (Figure 1). The basal T4 concentration did not differ between WT and *Thra1*$^{PV/+}$ mice, whereas T3 and TSH levels were increased in *Thra1*$^{PV/+}$ mice by 1.5-fold ($P <$ .01) and 6-fold ($P <$ .001), respectively. Thus, the characteristically reduced T4:T3 ratio identified in individuals with *THRA* mutations (5–7) was also present in *Thra1*$^{PV/+}$ mice (T4:T3 ratio: *Thra1*$^{PV/+}$ 23 vs WT 39). Supra-physiological T4 treatment completely suppressed TSH in both WT and *Thra1*$^{PV/+}$ mice. Despite profound and similar suppression of TSH, the increases in circulating T4 and T3 concentrations were attenuated in *Thra1*$^{PV/+}$ mice (T4 3.5-fold increase; T3 1.5-fold) compared to WT (T4 6-fold increase, $P <$ .001; T3 4-fold, $P <$ .01) indicating they are resistant to T4 administration.

Delayed ossification and impaired bone modeling in Thra1$^{PV/+}$ mice

Delayed bone development in juvenile *Thra1*$^{PV/+}$ mice (21) led to severe skeletal abnormalities in adults. Growth plates in 14 and 20 week-old *Thra1*$^{PV/+}$ mice were 39% and 70% wider than in WT mice (Figure 2A-B), demonstrating persistent delay of endochondral ossification. An increased degree of retention of mineralized cartilage within trabeculae revealed that bone modeling was also impaired (Figure 2C). T4 administration did not affect either of these abnormalities in mutant mice (Figure 2 and data not shown).

Structural consequences of defective ossification, modeling and remodeling in adult Thra1$^{PV/+}$ mice

Bones from 14 and 20 week-old *Thra1*$^{PV/+}$ mice were grossly dysmorphic. They were 17% and 15% shorter than WT and had splayed metaphyses, an abnormal cross-section throughout the diaphysis and misshapen joint surfaces (Figure 3A). Micro-CT analysis indicated that trabecular bone volume, number and thickness were increased in 20 week-old *Thra1*$^{PV/+}$ mice (BV/TV, 2.1 fold; Tb.N, 1.9 fold; Tb.Th, 1.1 fold greater) (Supplemental Figure 1) and these findings were confirmed by backscattered electron-scanning EM (BSE-SEM) (Figure 3B). Similarly, cortical bone thickness (48% wider at 14 weeks, 43% at 20 weeks) and periosteal diameter (13% larger at 14 weeks, 20% at 20 weeks) were markedly increased in *Thra1*$^{PV/+}$ mice (Supplemental Figure 1). T4 administration had no effect on these morphological abnormalities (Figure 3A), but resulted in a gradual increase in cortical bone thickness and diameter in *Thra1*$^{PV/+}$ mice (Supplemental Figure 1). Importantly, the endosteal diameter did not change in *Thra1*$^{PV/+}$ mice following T4 treatment,

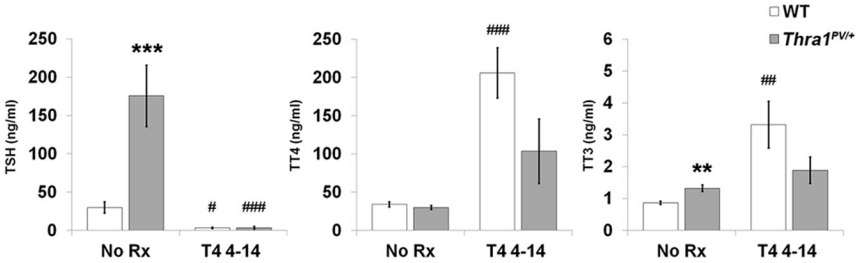

Figure 1. Thyroid status and response to T4 administration in *Thra1*$^{PV/+}$ mice Serum TSH (ng/ml), total T4 (ng/ml) and total T3 (ng/ml) concentrations in 14 week-old WT and *Thra1*$^{PV/+}$ mice (n = 5–13 per group) following treatment with vehicle (no Rx) or T4 between the ages of 4 and 14 weeks. Statistical comparisons: (i) WT vs *Thra1*$^{PV/+}$, student's *t* test, ** $P <$ .01, ***$P <$ .001; (ii) no Rx vs T4 treatment, student's *t* test, # $P <$ .05, ## $P <$ .01, ### $P <$ .001.

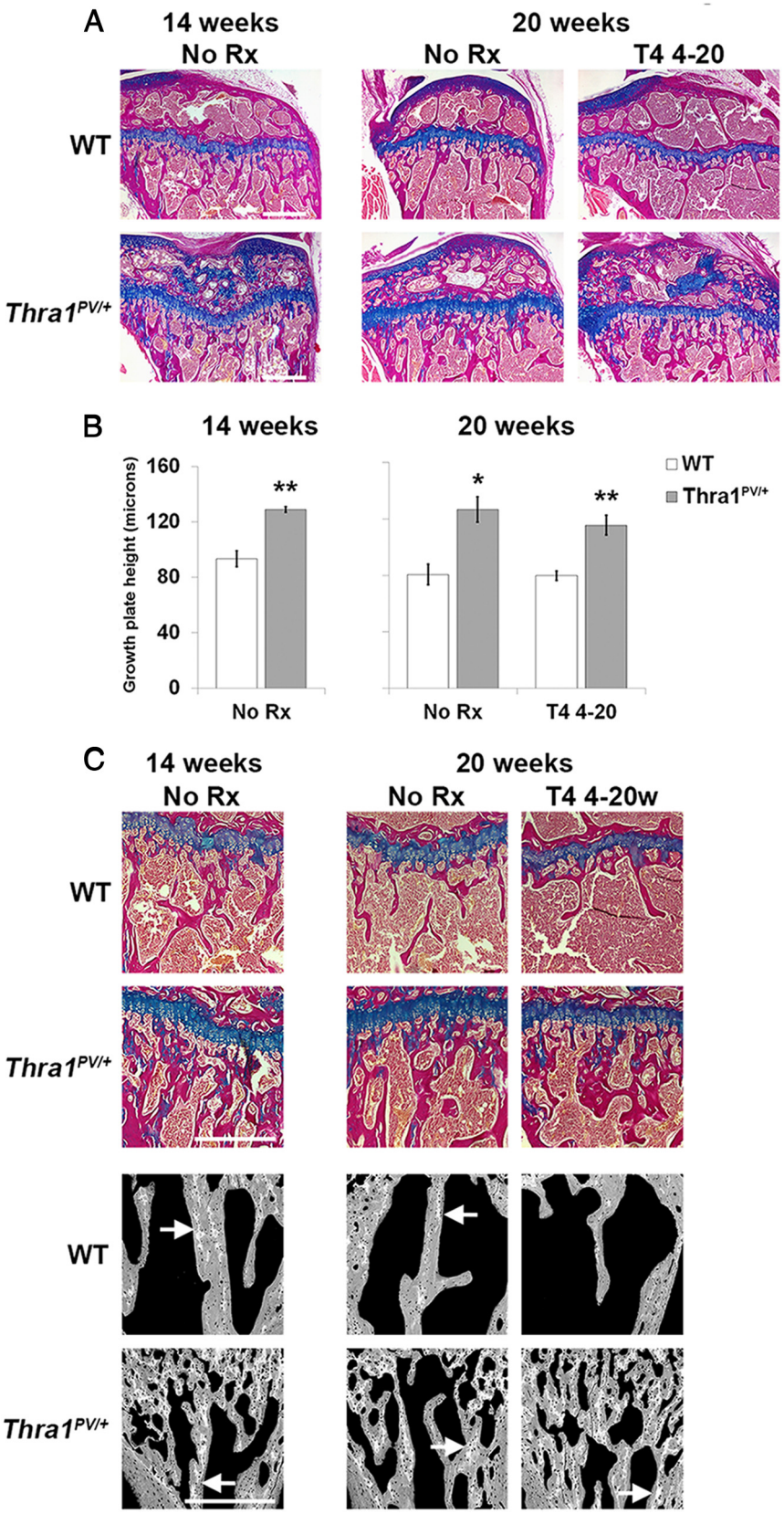

Figure 2. Effect of T4 treatment on the growth plate in *Thra1*$^{PV/+}$ mice **A.** Tibial growth plate sections stained with alcian blue (cartilage) and van Gieson (bone) from 14 and 20 week-old WT and *Thra1*$^{PV/+}$ mice treated with vehicle (no Rx) or T4. Bar = 500 μm. **B.** Growth plate heights (mean ± SEM) in 14 and 20 week-old mice (n = 3 per genotype per group).

whereas in WT mice it increased by 16% ($P < .01$). Thus, the increase in cortical bone thickness in *Thra1*$^{PV/+}$ mice resulted from a failure of endosteal bone resorption combined with a likely increase in periosteal bone deposition.

Increased bone mineral content but reduced mineralization in Thra1$^{PV/+}$ mice

X-ray microradiography revealed that 14 week-old *Thra1*$^{PV/+}$ mice had lower bone mineral content than WT mice, consistent with reduced mineral accrual during postnatal growth (21). Thus, in Figure 4A the pseudocolored images in 14 week-old mice show more yellow and fewer red pixels in *Thra1*$^{PV/+}$ mice compared to WT, indicating reduced bone mineral content. These differences are shown graphically in Figure 4B, in which the frequency distribution for *Thra1*$^{PV/+}$ mice is shifted to the left. By contrast, in 20 week-old mice there was a small shift to the right in the pixel frequency distribution for *Thra1*$^{PV/+}$ mice indicating higher, rather than lower, bone mineral content in older animals (Figure 4A-B). Remarkably, supra-physiological T4 treatment further increased bone mineral content in *Thra1*$^{PV/+}$ mice even though, as expected, it was reduced in WT mice following treatment (Figure 4A-B). Thus, *Thra1*$^{PV/+}$ mice were resistant to T4-induced bone loss, and had a paradoxical increase in bone mineral content following treatment. Despite this, BSE-SEM revealed that cortical and trabecular bone mineralization density was reduced in 20 week-old *Thra1*$^{PV/+}$ mice, the difference being greater in cortical bone, and that T4 treatment did not affect mineralization (Figure 5A-D). Thus, *Thra1*$^{PV/+}$ mice have an increase in bone mineral content (Figure 4) despite the reduction in tissue mineralization density (Figure 5) because

their trabecular and cortical bone volume is substantially increased (Figure 2 and Supplemental Figure 1). Overall, therefore, *Thra1*$^{PV/+}$ mice have increased cortical and trabecular bone volume compared to WT, but their bone is less mineralized.

Legend to Figure 2 Continued. . .
Statistical comparisons: 14 and 20 week-old mice, WT vs *Thra1*$^{PV/+}$, student's *t* test, * $P < .05$, ** $P < .01$. C. Panels show decalcified sections of tibial metaphysis stained with alcian blue and van Gieson from 14 and 20 week-old WT and *Thra1*$^{PV/+}$ mice (bar = 500 μm) and undecalcified sections of caudal vertebrae imaged by quantitative BSE-SEM (bar = 500 μm). White arrows show increased amounts of highly mineralized cartilage retained within trabecular bone in *Thra1*$^{PV/+}$ mice.

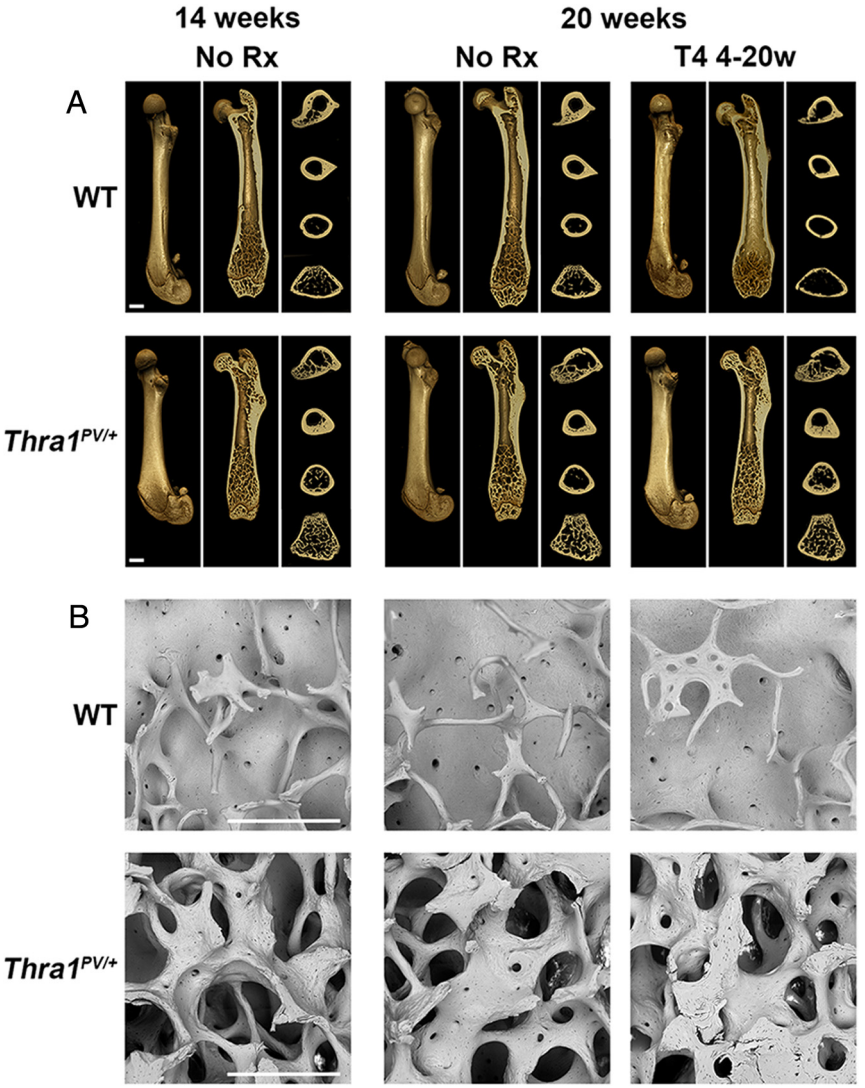

Figure 3. Effect of T4 treatment on bone structure in *Thra1*$^{PV/+}$ mice A. Micro-CT images of femurs from 14 and 20 week-old WT and *Thra1*$^{PV/+}$ mice following treatment with vehicle (no Rx) or T4. A longitudinal image of the bone surface, a midline section and transverse sections at four levels are shown. Bars = 1000 μm. **B.** BSE-SEM views of distal femur trabecular bone from 14 and 20 week-old WT and *Thra1*$^{PV/+}$ mice. Bars = 500 μm.

Reduced osteoclastic bone resorption in Thra1$^{PV/+}$ *mice*

Consistent with micro-CT and BSE-SEM analysis, histomorphometry studies demonstrated increased bone volume and surface in *Thra1*$^{PV/+}$ mice. Furthermore, osteoclast surfaces were reduced and fewer osteoclasts were present in *Thra1*$^{PV/+}$ mice compared to WT (Figure 6A-C). Thus, *Thra1*$^{PV/+}$ mice had a smaller proportion of their increased bone surface covered by osteoclasts (see also Supplemental Figure 2). The differences in bone surface, BV/TV, Oc.S/BS and Oc.N/BS between WT and *Thra1*$^{PV/+}$ mice were accentuated following T4 treatment (Figure 6A-C). Consistent with these findings, bone resorption was generally lower in *Thra1*$^{PV/+}$ mice (Supplemental Figure 2) but bone formation parameters were similar (Supplemental Figure 3). However, it is important to note that small differences in dynamic bone formation may not have been detected in these studies as only 3 mice were analyzed per group.

Abnormal bone stiffness and strength after prolonged T4 treatment of Thra1$^{PV/+}$ mice

Biomechanical testing revealed no difference in bone strength between untreated WT and *Thra1*$^{PV/+}$ mice (Figure 7A-B). Nevertheless, T4 treatment resulted in gradual increases in yield load, maximum load, fracture load and stiffness of bones from *Thra1*$^{PV/+}$ mice (Figure 7A-B). Thus, prolonged T4 administration abnormally and progressively increased bone stiffness and strength in *Thra1*$^{PV/+}$ mice.

Discussion

Skeletal phenotype resulting from mutation of Thra

During development *Thra1*$^{PV/+}$ mice have delayed closure of the skull sutures, severe growth retardation, delayed bone age and impaired bone mineral accrual (22). The de-

layed ossification persists into adulthood and is accompanied by impaired bone modeling and remodeling, resulting in; short stature, increased bone mass and gross morphological abnormalities of the bones and joints, but normal bone strength. These findings suggest that, despite severe skeletal abnormalities, adults with *THRA* mutations are unlikely to have an increased risk of fracture. However morphological abnormalities affecting the bones and joints predict they may be at increased risk of osteoarthritis (27, 28).

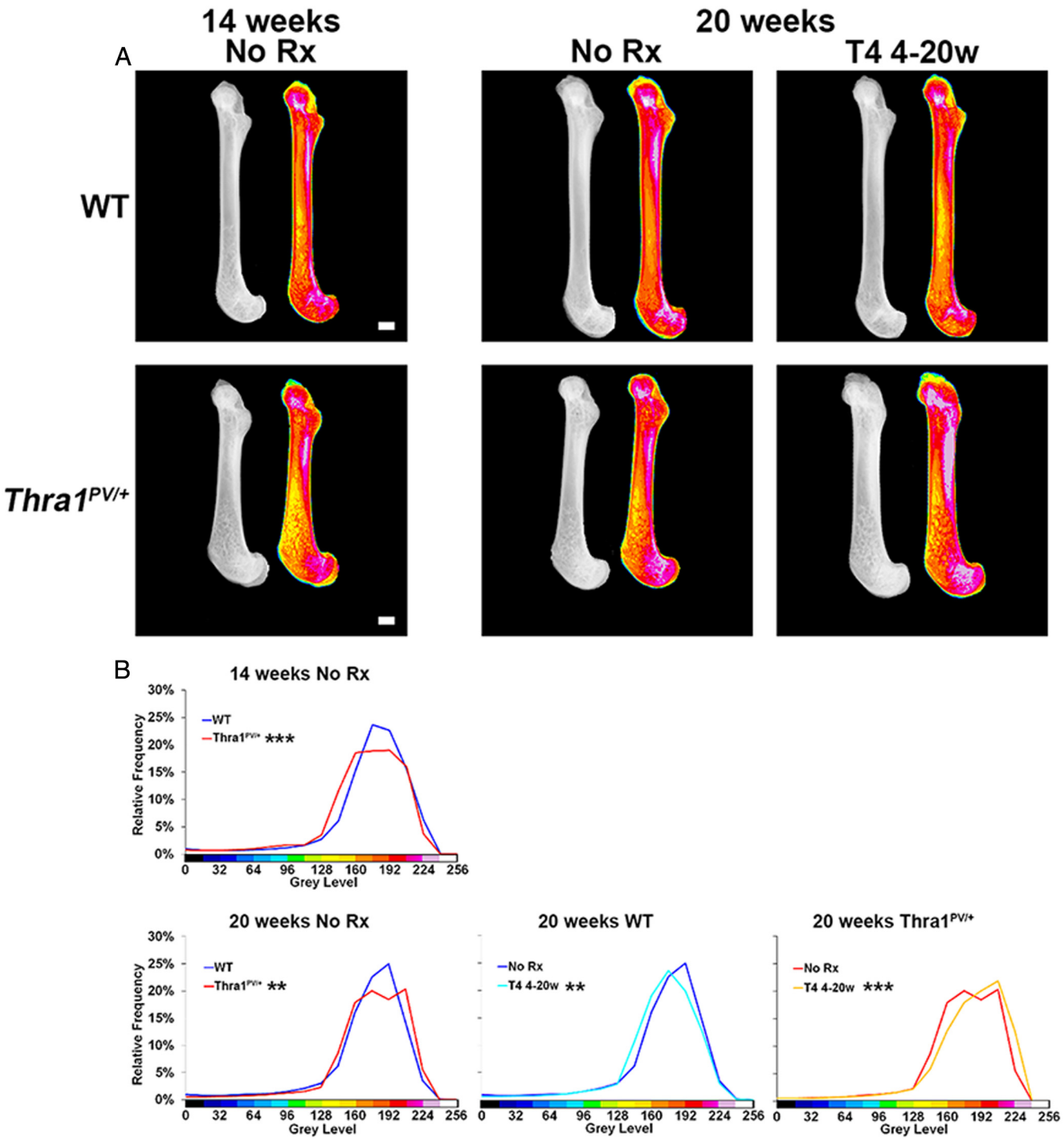

Figure 4. Effect of T4 treatment on bone mineral content in *Thra1*$^{PV/+}$ mice A. Quantitative Faxitron x-ray microradiography images of femurs from 14 and 20 week-old WT and *Thra1*$^{PV/+}$ mice following treatment with vehicle (no Rx) or T4. Gray-scale images were pseudocolored according to a 16-color palette in which low mineral content is blue-black and high mineral content is pink-white. Bars = 1000 μm. **B.** Relative frequency histograms of femur bone mineral content (n = 3 per genotype per group). Kolmogorov-Smirnov test, WT vs *Thra1*$^{PV/+}$ or no Rx vs T4 treatment, $^{**}P < .01$, $^{***}P < .001$.

Cellular and molecular mechanisms

The abnormalities in *Thra1*$^{PV/+}$ mice are consistent with effects of prolonged hypothyroidism on the growing and adult skeleton (38–42). Hypothyroidism disrupts growth plate chondrocyte differentiation leading to delayed endochondral ossification and linear growth, impairs bone modeling, and uncouples the processes of osteoclastic bone resorption and osteoblastic bone formation (43). In adults, even though it is well established that thyroid hormones increase bone resorption and promote bone loss, it is not known whether T3 acts directly in osteoclasts or whether effects on osteoclasts are secondary to the direct actions of T3 in osteoblasts (43). In *Thra1*$^{PV/+}$ mice, prolonged impairment of chondrocyte differentiation is manifest by growth retardation and short stature in adulthood. Similarly, defective osteoclastic bone resorption is evidenced by; reduced metaphyseal in-wasting, abnormal diaphyseal cross-section, and increased trabecular bone volume with retention of mineralized cartilage. Moreover, the grossly delayed formation of secondary ossification centers and reduced bone mineral accrual in *Thra1*$^{PV/+}$ mice persisted throughout growth when mice were active and gaining weight. Thus, unmineralized epiphyses were exposed to abnormal and greater mechanical loads, resulting in compensatory enlargement of the epiphyses and metaphyses, and culminating in adult joint deformity. Surprisingly, the strength of adult *Thra1*$^{PV/+}$ bones was normal despite these structural abnormalities and is accounted for by the increased cortical bone thickness and diameter (33, 44).

A series of studies in genetically modified mice have shown that TRα1 is the principal mediator of T3 action in bone and cartilage (12, 21, 45–48). The finding of an identical skeletal phenotype in patients with *THRA* mutations (5–7) now demonstrates that TRα1 has a similar essential role in human bone development. Analysis of the mechanisms underlying the skeletal phenotypes in *Thra* mutant mice revealed decreased expression of T3 target genes including growth hormone (GH) receptor (*Ghr*), insulin like growth factor-1 (*Igf1*), *Igf1* receptor (*Igf1r*), fibroblast growth factor receptor-1 (*Fgfr1*) and *Fgfr3*, and reduced downstream signaling responses mediated by the MAPK, STAT5 and AKT signaling pathways in chondrocytes and osteoblasts (12, 20, 21, 45, 49, 50). These data demonstrate impaired T3 action in cartilage and bone in *Thra* mutant mice despite a normal systemic T3 concentration, and thus indicate the skeletal phenotype in individuals with *THRA* mutations is a consequence of local resistance to thyroid hormone.

The phenotypes in *Thra1*$^{PV/+}$ mice and patients with *THRA* mutations result from the actions of potent dominant-negative mutant receptors. However, we have pre-

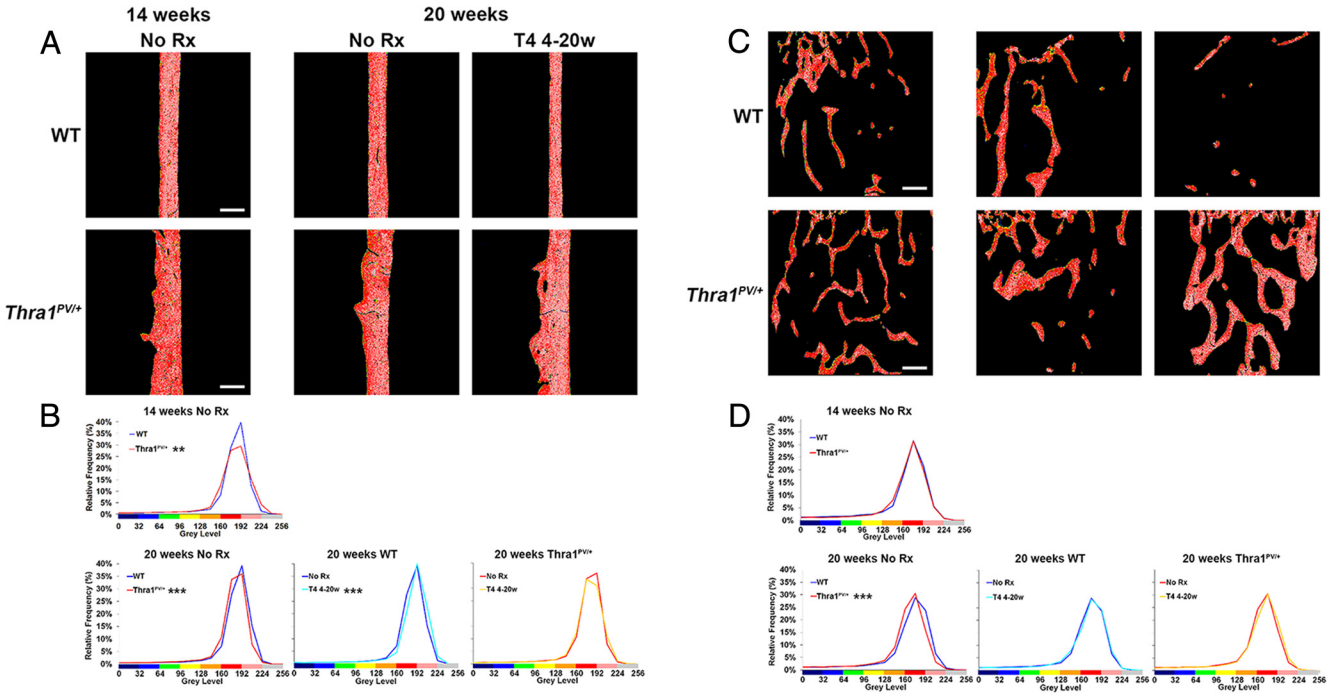

Figure 5. Effect of T4 treatment on bone mineralization density in *Thra1*$^{PV/+}$ mice **A.** Quantitative BSE-SEM images of femur mid-diaphysis cortical bone from 14 and 28 week-old WT and *Thra1*$^{PV/+}$ mice following treatment with vehicle (no Rx) or T4. Gray-scale images were pseudocolored according to an 8-color palette in which low mineral content is blue and high mineral content is pink-gray. Bars = 200 μm. **B.** Relative frequency histograms of cortical bone micromineralization densities (n = 3 per genotype per group). **C.** Images of distal femur trabecular bone Bars = 200 μm. **D.** Relative frequency histograms of trabecular bone micromineralization densities (n = 3 per genotype per group). Kolmogorov-Smirnov test, WT vs *Thra1*$^{PV/+}$ or no Rx vs T4 treatment, $^{**}P < .01$, $^{***}P < .001$.

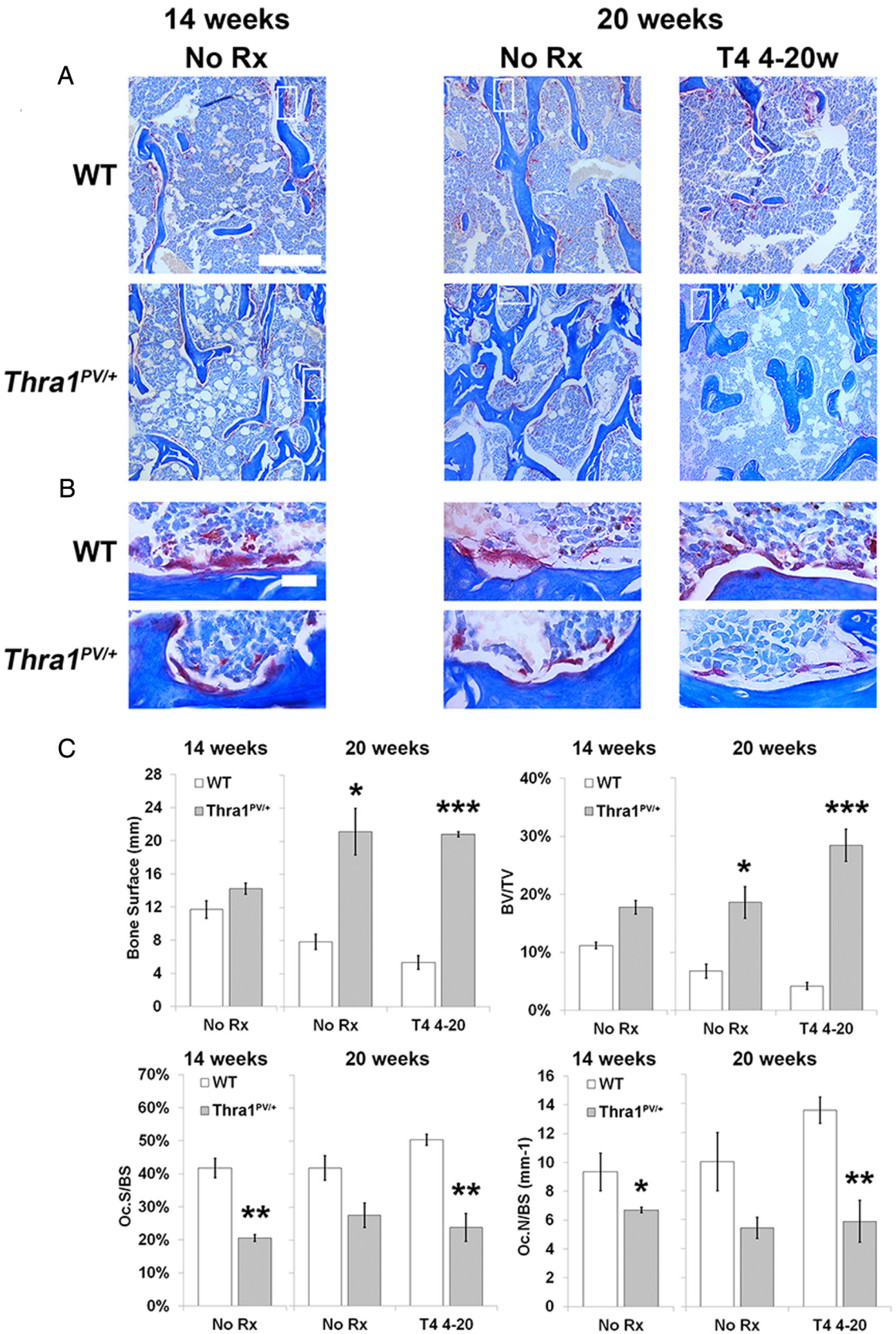

Figure 6. Effect of T4 treatment on osteoclastic bone resorption in *Thra1*$^{PV/+}$ mice **A.** Low power views (bar = 100 μm) of tibia trabecular bone from 14 and 20 week-old WT and *Thra1*$^{PV/+}$ mice following treatment with vehicle (no Rx) or T4, and stained for tartrate resistant acid phosphatase activity (pink) with aniline blue counterstain. The white boxes indicate the locations of the corresponding high power images shown in Panel B. **B.** High power views (bar = 10 μm) of osteoclasts lining trabecular bone surfaces. **C.** Quantitative analysis of bone surface,

viously reported that mice harboring a less severe $Thra1^{R384C}$ mutation have a milder phenotype with only transiently delayed ossification and growth retardation, although modeling and remodeling defects resulting in increased bone mass, cortical thickness and diameter were present in adults (45, 47). Importantly, and in contrast to $Thra1^{PV/+}$ mice, treatment of $Thra1^{R384C}$ mice with a dose of T3 that overcomes the reduced ligand binding affinity and dominant negative activity of the mutant receptor did ameliorate their skeletal abnormalities (45).

Therapeutic approaches in individuals with THRA mutations

The response to thyroid hormone treatment in $Thra1^{R384C}$ mice suggests that individuals with *THRA* mutations may benefit from similar treatment. Unfortunately, however, doses of T4 sufficient to normalize circulating hormone concentrations have been largely ineffective in the patients treated so far (5–8), presumably because the currently identified individuals have mutations that result in expression of mutant receptors with little or no T3 binding affinity. Despite this, Van Mullem et al showed that dominant-negative inhibition of TRβ by TR$\alpha 1^{F397fs406X}$ in vitro could be overcome partially by increasing concentrations of thyroid hormones (8). In this context, several studies have suggested that TRβ can mediate T3 action in bone and cartilage (9–12), even though the principal physiological effects are mediated via TRα1. Thus, we hypothesized that treatment of $Thra1^{PV/+}$ mice with a supra-physiological dose of T4 might improve bone structure and strength.

However, such treatment of $Thra1^{PV/+}$ mice had no beneficial effect on growth or skeletal deformity but did, nevertheless, increase cortical bone thickness and diameter. These responses were likely mediated by TRβ and resulted in abnormal increases in bone stiffness and strength that may adversely affect the optimal compromise between strength and flexibility that is essential to minimize fracture risk (51). Thus, prolonged treatment of individuals harboring *THRA* mutations with high doses of T4 may also have adverse consequences in other tissues where T3 action is predominantly mediated via TRβ.

Growth hormone therapy (HT) represents an alternative approach to improve linear growth and skeletal maturation in children with *THRA* mutations, but treatment in one individual so far was ineffective (6). The reduced expression of *Ghr*, *Igf1* and *Igf1r*, together with impaired STAT5 and AKT signaling in growth plate chondrocytes in *Thra* mutant mice (12, 21, 50), suggests a mechanism to account for this lack of clinical response to GH.

Thyroid hormone metabolism and response to T4 administration in $Thra1^{PV/+}$ mice

Thyroid hormone metabolism is mediated by three iodothyronine deiodinases. The type 1 enzyme (D1) catalyzes removal of an inner or outer ring iodine from T4 to generate T3 or reverse T3 (rT3), or an outer ring iodine from rT3 to generate 3,3′- diiodothyronine (T2). D1 is expressed in liver, kidney and thyroid and contributes to the circulating concentration of T3 (52). The type 2 enzyme (D2) converts the prohormone T4 to the active hormone T3: it is expressed in the hypothalamus and pituitary and peripheral target tissues, where it generates a local supply of T3 and is subject to substrate-mediated inactivation (53). By contrast, the type 3 enzyme (D3) catalyzes removal of an inner ring iodine from T4 or T3 to generate the inactive metabolites rT3 or T2. D3 expression is induced by thyroid hormone, thus limiting the supply of T3 in conditions of thyroid hormone excess (52).

Remarkably, and despite complete suppression of TSH, $Thra1^{PV/+}$ mice had a blunted increase in circulating thyroid hormones following a supra-physiological dose of T4. This discrepancy indicates that the HPT axis is intact in $Thra1^{PV/+}$ mice but metabolism of thyroid hormones must be increased. Indeed, we previously showed that untreated $Thra1^{PV/+}$ mice have a 9-fold increase in hepatic D1 mRNA expression (14) resulting in a 4.8-fold increase in enzyme activity (54). It is well established that T3 acts via TRβ1 to stimulate D1 expression in the liver (55, 56) and accordingly hepatic D1 activity is increased further in $Thra1^{PV/+}$ mice following treatment with T3 (54, 57). By contrast, T3 acts via TRα1 to stimulate expression of D3 (58) and we previously demonstrated that T3 treatment of $Thra1^{PV/+}$ mice fails to induce the normal increase in D3 activity observed in WT animals (54, 57).

We propose, therefore, that the resistance to T4 administration observed in $Thra1^{PV/+}$ mice results from the markedly increased D1 activity combined with this absent D3 response (Figure 8). Consistent with this model, TSH in individuals with *THRA* mutations was suppressed readily following T4 treatment despite only small increases in T4 and T3 concentrations (7, 8). Detailed future metabolic studies will be required to confirm the precise underlying mechanisms responsible for these findings. For

Legend to Figure 6 Continued. . .
bone volume per tissue volume (BV/TV), osteoclast surface per bone surface (Oc.S/BS) and osteoclast number per bone surface (Oc.N/BS) (mean ± SEM) in 14 and 20 week-old mice, (n = 3 per genotype per group). Statistical comparisons: 14 and 20 week-old mice, WT vs $Thra1^{PV/+}$, student's *t* test, * $P < .05$, ** $P < .01$, *** $P < .001$.

example, as defects in TRα1 action may result in intestinal problems, it is possible that absorption of orally administered T4 could be impaired in *Thra1*$^{PV/+}$ mice. However, it should also be noted that, following oral treatment with T4, the TSH concentration was suppressed completely in both WT and *Thra1*$^{PV/+}$ mice, indicating intestinal ab-

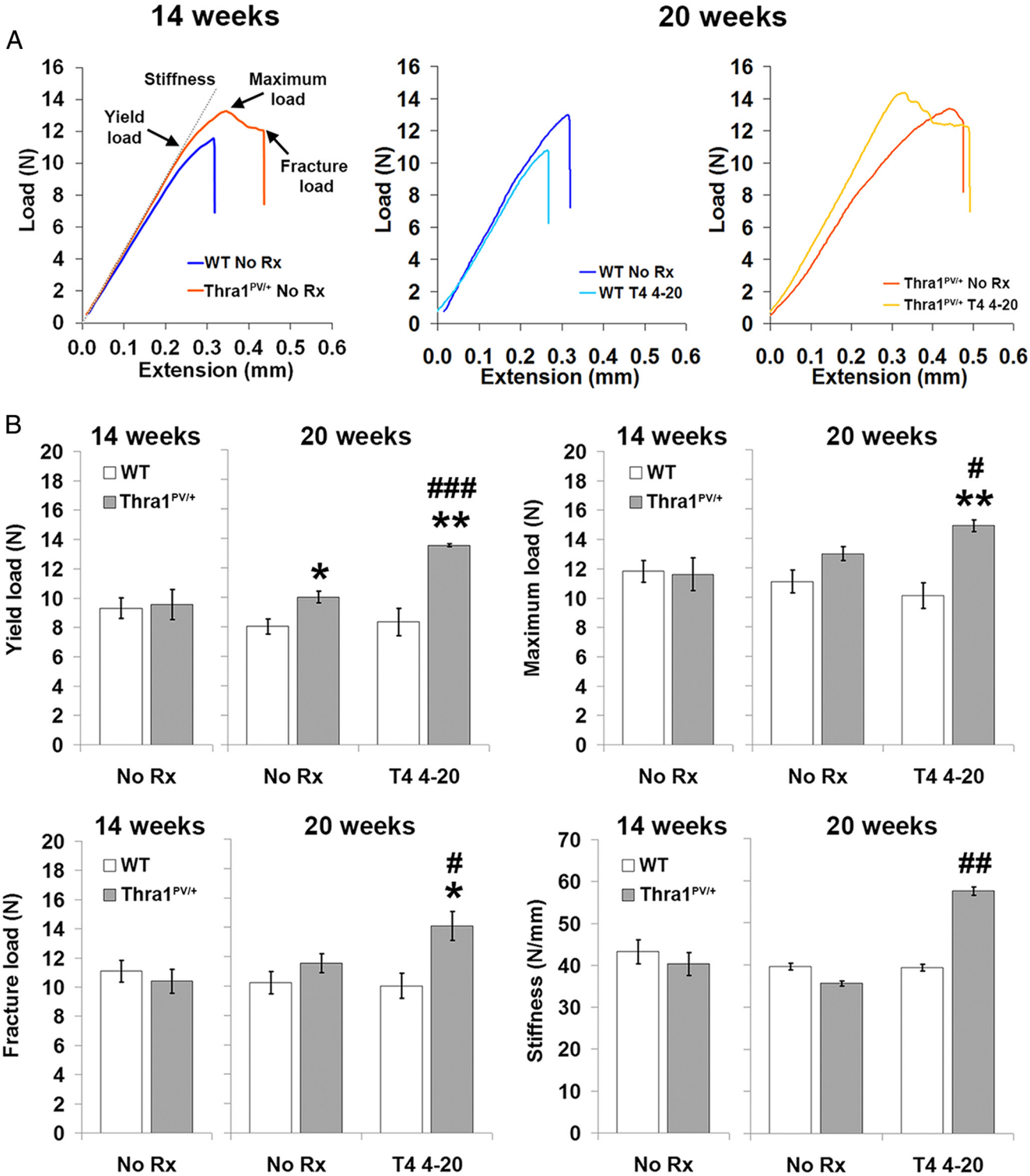

Figure 7. Effect of T4 treatment on cortical bone strength in *Thra1*$^{PV/+}$ mice **A.** Representative load-displacement curves from destructive 3 point bend testing of tibias from 14 and 20 week-old WT and *Thra1*$^{PV/+}$ mice following treatment with vehicle (no Rx) or T4. **B.** Quantitative analysis of yield load, maximum load, fracture load and stiffness (mean ± SEM) in 14 and 20 week-old mice (n = 3 per genotype per group). Statistical comparisons: (i) 14 and 20 week-old mice, WT vs *Thra1*$^{PV/+}$, student's *t* test, * $P < .05$; (ii) 20 week-old mice, no Rx vs T4 treatment from 4–20 weeks, student's *t* test, # $P < .05$, ## $P < .01$, ### $P < .001$.

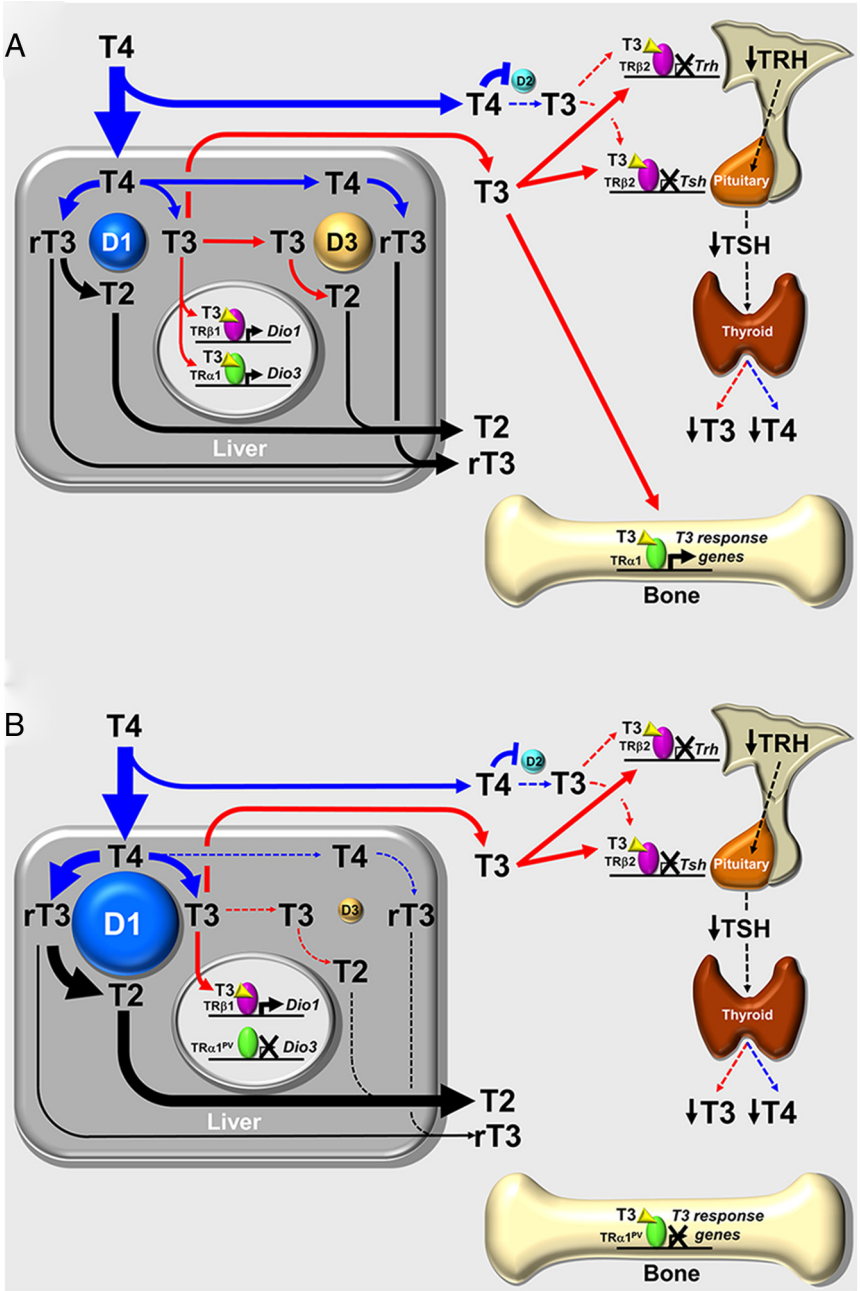

Figure 8. Proposed model for attenuated systemic response to T4 administration in *Thra1*$^{PV/+}$ mice **A.** Normal response in WT mice. High concentrations of T4 are metabolized in the liver. D1 converts T4 to rT3 or T3, and rT3 is metabolized to T2. Acting via TRβ1, T3 increases D1 expression to complete a feed-forward loop. However, T3 also acts via TRα1 to increase D3 expression and thus limit feed-forward activation of D1. Thus, T4 excess results in a parallel increase in both D1 and D3 so that levels of T3, rT3 and T2 in the circulation rise to reflect increased T4 metabolism. The high levels of circulating thyroid hormones suppress TRH and TSH expression and inhibit endogenous T4 and T3 production. At steady state, most circulating T3 is derived from increased D1-mediated metabolism of T4. The TRα1-mediated actions of T3 in bone are increased. **B.** Abnormal response in *Thra1*$^{PV/+}$ mice. High concentrations of T4 are metabolized in the liver. D1 converts T4 to rT3 or T3, and rT3 is metabolized to T2. Acting via TRβ1, T3 increases D1 expression to complete a feed-forward loop. However, in *Thra1*$^{PV/+}$ mice the mutant TRα1^{PV} prevents T3 stimulation of D3 expression, thus maintaining feed-forward activation of D1. Administration of T4 fuels this feed-forward activation and would result in enhanced metabolism of T4, and ultimately increased accumulation of T2. Thus, although circulating T3 and T4 levels rise to a lesser degree than in WT animals, they are still sufficient to suppress the hypothalamus-pituitary-thyroid axis. At steady state, the grossly increased D1 activity thus accounts for resistance of *Thra1*$^{PV/+}$ mice to T4 sorption of T4 was unlikely to be markedly impaired in *Thra1*$^{PV/+}$ mice. Nevertheless, it would be instructive to investigate whether differences in serum T4 and T3 levels persist between WT and *Thra1*$^{PV/+}$ mice following parenteral administration of T4.

Conclusions

The overall resistance of the skeleton to T4 treatment in *Thra1*$^{PV/+}$ mice and the patients studied so far is likely to be a consequence of the potent dominant-negative activities of their mutant TRα1 proteins (5–7, 14, 18). It is inevitable, however, that individuals with less severe *THRA* mutations will be identified in the future and in such cases T4 treatment is likely to be beneficial. Thus, treatment of *Thra1*^{R384C} mice with doses of T4 that overcome the reduced binding affinity of TRα1^{R384C} rescued their skeletal phenotype by preventing delayed ossification and growth retardation, ultimately ameliorating adult bone structure and mineralization (45). Taken together, these studies predict that individuals with *THRA* mutations will display variable degrees of skeletal deformity and different responses to T4 treatment that correlate with the functional consequences of the particular disease causative mutation. Therefore, in patients with *THRA* mutations, it will be important to characterize the functional properties of their mutant TRα1 as this may predict their response to T4 treatment and the optimal systemic T4 concentration required.

Acknowledgments

We thank Maureen Arora for SEM sample preparation.

*Address all correspondence and requests for reprints to: Graham R. Williams, Molecular Endocrinology Group, Imperial College London, 7N2a Commonwealth Building, Hammersmith Campus, Du Cane Road, London, W12 0NN, UK Tel: +44 208 383 1383; email: graham.williams@imperial.ac.uk.

Disclosure Summary: The authors have nothing to disclose

Sheue-yann Cheng, Gene Regulation Section, Laboratory of Molecular Biology, National Cancer Institute, National Institutes of Health, Bethesda, MD 20892–4264, USA Tel: 301 496 4280; email: chengs@mail.nih.gov

This work was supported by Medical Research Council Research Grants (JHDB and GRW); Intramural Research Program, NCI, NIH (S-yC); Ernest Heine Family Foundation and Mrs Janice Gibson (PIC).

References

1. **Cheng SY, Leonard JL, Davis PJ.** Molecular aspects of thyroid hormone actions. *Endocr Rev*. 2010;31(2):139–170.
2. **Refetoff S, DeWind LT, DeGroot LJ.** Familial syndrome combining deaf-mutism, stuppled epiphyses, goiter and abnormally high PBI: possible target organ refractoriness to thyroid hormone. *J Clin Endocrinol Metab*. 1967;27(2):279–294.
3. **Sakurai A, Takeda K, Ain K, Ceccarelli P, Nakai A, Seino S, Bell GI, Refetoff S, DeGroot LJ.** Generalized resistance to thyroid hormone associated with a mutation in the ligand-binding domain of the human thyroid hormone receptor beta. *Proc Natl Acad Sci U S A*. 1989;86(22):8977–8981.
4. **Dumitrescu AM, Refetoff S.** The syndromes of reduced sensitivity to thyroid hormone. *Biochim Biophys Acta*. 2012;1830(7):3987–4003.
5. **Bochukova E, Schoenmakers N, Agostini M, Schoenmakers E, Rajanayagam O, Keogh JM, Henning E, Reinemund J, Gevers E, Sarri M, Downes K, Offiah A, Albanese A, Halsall D, Schwabe JW, Bain M, Lindley K, Muntoni F, Vargha-Khadem F, Dattani M, Farooqi IS, Gurnell M, Chatterjee K.** A mutation in the thyroid hormone receptor alpha gene. *New Engl J Med*. 2012;366(3):243–249.
6. **van Mullem A, van Heerebeek R, Chrysis D, Visser E, Medici M, Andrikoula M, Tsatsoulis A, Peeters R, Visser TJ.** Clinical phenotype and mutant TRalpha1. *New Engl J Med*. 2012;366(15):1451–1453.
7. **Moran C, Schoenmakers N, Agostini M, Schoenmakers E, Offiah A, Kydd A, Kahaly G, Mohr-Kahaly S, Rajanayagam O, Lyons G, Wareham N, Halsall D, Dattani M, Hughes S, Gurnell M, Park SM, Chatterjee K.** An Adult Female With Resistance to Thyroid Hormone Mediated by Defective Thyroid Hormone Receptor alpha. *J Clin Endocrinol Metab*. 2013;98(11):4254–4261.
8. **van Mullem AA, Chrysis D, Eythimiadou A, Chroni E, Tsatsoulis A, de Rijke YB, Visser WE, Visser TJ, Peeters RP.** Clinical phenotype of a new type of thyroid hormone resistance caused by a mutation of the TRalpha1 receptor: consequences of LT4 treatment. *J Clin Endocrinol Metab*. 2013;98(7):3029–3038.
9. **Freitas FR, Capelo LP, O'Shea PJ, Jorgetti V, Moriscot AS, Scanlan TS, Williams GR, Zorn TM, Gouveia CH.** The thyroid hormone receptor beta-specific agonist GC-1 selectively affects the bone development of hypothyroid rats. *J Bone Miner Res*. 2005;20(2):294–304.
10. **Monfoulet LE, Rabier B, Dacquin R, Anginot A, Photsavang J, Jurdic P, Vico L, Malaval L, Chassande O.** Thyroid hormone receptor beta mediates thyroid hormone effects on bone remodeling and bone mass. *J Bone Miner Res*. 2011;26(9):2036–2044.
11. **Rabier B, Williams AJ, Mallein-Gerin F, Williams GR, Chassande O.** Thyroid hormone-stimulated differentiation of primary rib chondrocytes in vitro requires thyroid hormone receptor beta. *J Endocrinol*. 2006;191(1):221–228.
12. **Bassett JH, O'Shea PJ, Sriskantharajah S, Rabier B, Boyde A, Howell PG, Weiss RE, Roux JP, Malaval L, Clement-Lacroix P, Samarut J, Chassande O, Williams GR.** Thyroid hormone excess rather than thyrotropin deficiency induces osteoporosis in hyperthyroidism. *Mol Endocrinol*. 2007;21(5):1095–1107.
13. **Kaneshige M, Kaneshige K, Zhu X, Dace A, Garrett L, Carter TA, Kazlauskaite R, Pankratz DG, Wynshaw-Boris A, Refetoff S, Weintraub B, Willingham MC, Barlow C, Cheng S.** Mice with a targeted mutation in the thyroid hormone beta receptor gene exhibit impaired growth and resistance to thyroid hormone. *Proc Natl Acad Sci U S A*. 2000;97(24):13209–13214.
14. **Kaneshige M, Suzuki H, Kaneshige K, Cheng J, Wimbrow H, Barlow C, Willingham MC, Cheng S.** A targeted dominant negative mutation of the thyroid hormone alpha 1 receptor causes increased mortality, infertility, and dwarfism in mice. *Proc Natl Acad Sci U S A*. 2001;98(26):15095–15100.
15. **Parrilla R, Mixson AJ, McPherson JA, McClaskey JH, Weintraub BD.** Characterization of seven novel mutations of the c-erbA beta gene in unrelated kindreds with generalized thyroid hormone resistance. Evidence for two "hot spot" regions of the ligand binding domain. *J Clin Invest*. 1991;88(6):2123–2130.
16. **Cheng SY.** Thyroid hormone receptor mutations and disease: insights from knock-in mouse models. *Expert Rev Endocrinol Metab*. 2007;2(1):47–57.
17. **Barettino D, Vivanco Ruiz MM, Stunnenberg HG.** Characterization of the ligand-dependent transactivation domain of thyroid hormone receptor. *EMBO J*. 1994;13(13):3039–3049.
18. **Fozzatti L, Lu C, Kim DW, Cheng SY.** Differential recruitment of nuclear coregulators directs the isoform-dependent action of mutant thyroid hormone receptors. *Mol Endocrinol*. 2011;25(6):908–921.
19. **Fozzatti L, Lu C, Kim DW, Park JW, Astapova I, Gavrilova O, Willingham MC, Hollenberg AN, Cheng SY.** Resistance to thyroid hormone is modulated in vivo by the nuclear receptor corepressor (NCOR1). *Proc Natl Acad Sci U S A*. 2011;108(42):17462–17467.
20. **Stevens DA, Harvey CB, Scott AJ, O'Shea PJ, Barnard JC, Williams AJ, Brady G, Samarut J, Chassande O, Williams GR.** Thyroid hormone activates fibroblast growth factor receptor-1 in bone. *Mol Endocrinol*. 2003;17(9):1751–1766.
21. **O'Shea PJ, Bassett JH, Sriskantharajah S, Ying H, Cheng SY, Williams GR.** Contrasting skeletal phenotypes in mice with an identical mutation targeted to thyroid hormone receptor alpha1 or beta. *Mol Endocrinol*. 2005;19(12):3045–3059.
22. **O'Shea PJ, Bassett JH, Cheng SY, Williams GR.** Characterization of skeletal phenotypes of TRalpha1 and TRbeta mutant mice: implications for tissue thyroid status and T3 target gene expression. *Nucl Recept Signal*. 2006;4:e011.
23. **Meulenbelt I, Bos SD, Chapman K, van der Breggen R, Houwing-Duistermaat JJ, Kremer D, Kloppenburg M, Carr A, Tsezou A, Gonzalez A, Loughlin J, Slagboom PE.** Meta-analyses of genes modulating intracellular T3 bio-availability reveal a possible role for the DIO3 gene in osteoarthritis susceptibility. *Ann Rheum Dis*. 2011;70(1):164–167.
24. **Meulenbelt I, Min JL, Bos S, Riyazi N, Houwing-Duistermaat JJ, van der Wijk HJ, Kroon HM, Nakajima M, Ikegawa S, Uitterlinden AG, van Meurs JB, van der Deure WM, Visser TJ, Seymour AB, Lakenberg N, van der Breggen R, Kremer D, van Duijn CM, Kloppenburg M, Loughlin J, Slagboom PE.** Identification of DIO2 as a new

Legend to Figure 8 Continued. . .
administration. Despite exogenous thyroid hormone administration, T3 action in bone remains inhibited by dominant-negative TR$\alpha 1^{PV}$ (21).

susceptibility locus for symptomatic osteoarthritis. *Hum Mol Genet*. 2008;17(12):1867–1875.
25. **Murphy E, Gluer CC, Reid DM, Felsenberg D, Roux C, Eastell R, Williams GR.** Thyroid function within the upper normal range is associated with reduced bone mineral density and an increased risk of nonvertebral fractures in healthy euthyroid postmenopausal women. *J Clin Endocrinol Metab*. 2010;95(7):3173–3181.
26. **Vestergaard P, Mosekilde L.** Fractures in patients with hyperthyroidism and hypothyroidism: a nationwide follow-up study in 16,249 patients. *Thyroid*. 2002;12(5):411–419.
27. **Castano-Betancourt MC, Van Meurs JB, Bierma-Zeinstra S, Rivadeneira F, Hofman A, Weinans H, Uitterlinden AG, Waarsing JH.** The contribution of hip geometry to the prediction of hip osteoarthritis. *Osteoarthritis Cartilage*. 2013;21(10):1530–1536.
28. **Neogi T, Bowes MA, Niu J, De Souza KM, Vincent GR, Goggins J, Zhang Y, Felson DT.** Magnetic resonance imaging-based three-dimensional bone shape of the knee predicts onset of knee osteoarthritis: data from the osteoarthritis initiative. *Arthritis Rheum*. 2013;65(8):2048–2058.
29. **Bassett JH, Logan JG, Boyde A, Cheung MS, Evans H, Croucher P, Sun XY, Xu S, Murata Y, Williams GR.** Mice lacking the calcineurin inhibitor Rcan2 have an isolated defect of osteoblast function. *Endocrinology*. 2012;153(7):3537–3548.
30. **Pohlenz J, Maqueem A, Cua K, Weiss RE, Van Sande J, Refetoff S.** Improved radioimmunoassay for measurement of mouse thyrotropin in serum: strain differences in thyrotropin concentration and thyrotroph sensitivity to thyroid hormone. *Thyroid*. 1999;9(12):1265–1271.
31. **Barca-Mayo O, Liao XH, DiCosmo C, Dumitrescu A, Moreno-Vinasco L, Wade MS, Sammani S, Mirzapoiazova T, Garcia JG, Refetoff S, Weiss RE.** Role of type 2 deiodinase in response to acute lung injury (ALI) in mice. *Proc Natl Acad Sci U S A*. 2011;108(49):E1321–1329.
32. **Bianco AC, Anderson G, Forrest D, Galton VA, Gereben B, Kim BW, Kopp PA, Liao XH, Obregon MJ, Peeters RP, Refetoff S, Sharlin DS, Simonides WS, Weiss RE, Williams GR.** American thyroid association guide to investigating thyroid hormone economy and action in rodent and cell models. *Thyroid*. 2014;24(1):88–168.
33. **Bassett JH, Boyde A, Howell PG, Bassett RH, Galliford TM, Archanco M, Evans H, Lawson MA, Croucher P, St Germain DL, Galton VA, Williams GR.** Optimal bone strength and mineralization requires the type 2 iodothyronine deiodinase in osteoblasts. *Proc Natl Acad Sci U S A*. 2010;107(16):7604–7609.
34. **Bassett JH, van der Spek A, Gogakos A, Williams GR.** Quantitative X-ray imaging of rodent bone by Faxitron. *Methods Mol Biol*. 2012;816:499–506.
35. **Boyde A, Jones SJ, Aerssens J, Dequeker J.** Mineral density quantitation of the human cortical iliac crest by backscattered electron image analysis: variations with age, sex, and degree of osteoarthritis. *Bone*. 1995;16(6):619–627.
36. **Doube M, Firth EC, Boyde A.** Variations in articular calcified cartilage by site and exercise in the 18-month-old equine distal metacarpal condyle. *Osteoarthritis Cartilage*. 2007;15(11):1283–1292.
37. **Schriefer JL, Robling AG, Warden SJ, Fournier AJ, Mason JJ, Turner CH.** A comparison of mechanical properties derived from multiple skeletal sites in mice. *J Biomech*. 2005;38(3):467–475.
38. **Eriksen EF, Mosekilde L, Melsen F.** Kinetics of trabecular bone resorption and formation in hypothyroidism: evidence for a positive balance per remodeling cycle. *Bone*. 1986;7(2):101–108.
39. **Rivkees SA, Bode HH, Crawford JD.** Long-term growth in juvenile acquired hypothyroidism: the failure to achieve normal adult stature. *New Engl J Med*. 1988;318(10):599–602.
40. **Salerno M, Micillo M, Di Maio S, Capalbo D, Ferri P, Lettiero T, Tenore A.** Longitudinal growth, sexual maturation and final height in patients with congenital hypothyroidism detected by neonatal screening. *Eur J Endocrinol*. 2001;145(4):377–383.
41. **Mosekilde L, Melsen F.** Effect of antithyroid treatment on calcium-phosphorus metabolism in hyperthyroidism. II: Bone histomorphometry. *Acta endocrinol*. 1978;87(4):751–758.
42. **Mosekilde L, Melsen F.** Morphometric and dynamic studies of bone changes in hypothyroidism. *Acta Pathol Microbiol Scand A*. 1978;86(1):56–62.
43. **Waung JA, Bassett JH, Williams GR.** Thyroid hormone metabolism in skeletal development and adult bone maintenance. *Trends Endocrinol Metab*. 2012;23(4):155–162.
44. **Ritchie RO, Koester KJ, Ionova S, Yao W, Lane NE, Ager JW, 3rd.** Measurement of the toughness of bone: a tutorial with special reference to small animal studies. *Bone*. 2008;43(5):798–812.
45. **Bassett JH, Nordstrom K, Boyde A, Howell PG, Kelly S, Vennstrom B, Williams GR.** Thyroid status during skeletal development determines adult bone structure and mineralization. *Mol Endocrinol*. 2007;21(8):1893–1904.
46. **Gauthier K, Plateroti M, Harvey CB, Williams GR, Weiss RE, Refetoff S, Willott JF, Sundin V, Roux JP, Malaval L, Hara M, Samarut J, Chassande O.** Genetic analysis reveals different functions for the products of the thyroid hormone receptor alpha locus. *Mol Cell Biol*. 2001;21(14):4748–4760.
47. **Tinnikov A, Nordstrom K, Thoren P, Kindblom JM, Malin S, Rozell B, Adams M, Rajanayagam O, Pettersson S, Ohlsson C, Chatterjee K, Vennstrom B.** Retardation of post-natal development caused by a negatively acting thyroid hormone receptor alpha1. *EMBO J*. 2002;21(19):5079–5087.
48. **Gothe S, Wang Z, Ng L, Kindblom JM, Barros AC, Ohlsson C, Vennstrom B, Forrest D.** Mice devoid of all known thyroid hormone receptors are viable but exhibit disorders of the pituitary-thyroid axis, growth, and bone maturation. *Genes Dev*. 1999;13(10):1329–1341.
49. **Barnard JC, Williams AJ, Rabier B, Chassande O, Samarut J, Cheng SY, Bassett JH, Williams GR.** Thyroid hormones regulate fibroblast growth factor receptor signaling during chondrogenesis. *Endocrinology*. 2005;146(12):5568–5580.
50. **Xing W, Govoni KE, Donahue LR, Kesavan C, Wergedal J, Long C, Bassett JH, Gogakos A, Wojcicka A, Williams GR, Mohan S.** Genetic evidence that thyroid hormone is indispensable for prepubertal insulin-like growth factor-I expression and bone acquisition in mice. *J Bone Miner Res*. 2012;27(5):1067–1079.
51. **Bassett JH, Gogakos A, White JK, Evans H, Jacques RM, van der Spek AH, Sanger Mouse Genetics P, Ramirez-Solis R, Ryder E, Sunter D, Boyde A, Campbell MJ, Croucher PI, Williams GR.**. Rapid-throughput skeletal phenotyping of 100 knockout mice identifies 9 new genes that determine bone strength. *PLoS Genet*. 2012;8(8):e1002858.
52. **Bianco AC, Kim BW.** Deiodinases: implications of the local control of thyroid hormone action. *J Clin Invest*. 2006;116(10):2571–2579.
53. **Dentice M, Bandyopadhyay A, Gereben B, Callebaut I, Christoffolete MA, Kim BW, Nissim S, Mornon JP, Zavacki AM, Zeold A, Capelo LP, Curcio-Morelli C, Ribeiro R, Harney JW, Tabin CJ, Bianco AC.** The Hedgehog-inducible ubiquitin ligase subunit WSB-1 modulates thyroid hormone activation and PTHrP secretion in the developing growth plate. *Nat Cell Biol*. 2005;7(7):698–705.
54. **Zavacki AM, Ying H, Christoffolete MA, Aerts G, So E, Harney JW, Cheng SY, Larsen PR, Bianco AC.** Type 1 iodothyronine deiodinase is a sensitive marker of peripheral thyroid status in the mouse. *Endocrinology*. 2005;146(3):1568–1575.
55. **Amma LL, Campos-Barros A, Wang Z, Vennstrom B, Forrest D.** Distinct tissue-specific roles for thyroid hormone receptors beta and alpha1 in regulation of type 1 deiodinase expression. *Mol Endocrinol*. 2001;15(3):467–475.
56. **Gullberg H, Rudling M, Forrest D, Angelin B, Vennstrom B.** Thyroid hormone receptor beta-deficient mice show complete loss of the normal cholesterol 7alpha-hydroxylase (CYP7A) response to thyroid hormone but display enhanced resistance to dietary cholesterol. *Mol Endocrinol*. 2000;14(11):1739–1749.
57. **Zavacki AM, Larsen PR.** RTHalpha, a newly recognized phenotype

of the resistance to thyroid hormone (RTH) syndrome in patients with THRA gene mutations. *J Clin Endocrinol Metab*. 2013;98(7):2684–2686.

58. **Barca-Mayo O, Liao XH, Alonso M, Di Cosmo C, Hernandez A, Refetoff S, Weiss RE.** Thyroid hormone receptor alpha and regulation of type 3 deiodinase. *Mol Endocrinol*. 2011;25(4):575–583.